A Novel Functional Neuron Group for Respiratory Rhythm Generation in the Ventral Medulla

Hiroshi Onimaru and Ikuo Homma
Showa University School of Medicine, Shinagawa-ku, Tokyo 142-8555, Japan

We visualized respiratory neuron activity covering the entire ventral medulla using optical recordings in a newborn rat brainstem–spinal cord preparation stained with voltage-sensitive dye. We measured optical signals from several seconds before to several seconds after the inspiratory phase using the inspiratory motor nerve discharge as the trigger signal; we averaged the optical signals of 50–150 respiratory cycles to obtain an optical image correlating particularly to inspiratory activity. The optical images we obtained from the ventral approach indicated that neuron activity first appeared during the respiratory cycle in the limited region of the rostral ventrolateral medulla (RVLM), preceding the onset of inspiratory activity by ~500 msec. During the inspiratory phase, plateau activity appeared in the more caudal ventrolateral medulla at the level of the most rostral roots of the XIIth nerve. Comparison with electrophysiological recordings from respiratory neurons in the RVLM suggested that the optical signals preceding the inspiratory burst reflect preinspiratory neuron activity in this area. This RVLM area was determined to be ventrolateral to the facial nucleus and close to the ventral surface. We referred to this functional neuron group as the para-facial respiratory group (pFRG). Partial, bilateral electrical lesioning of the pFRG significantly reduced the respiratory frequency, together with changes in the spatiotemporal pattern of respiratory neuron activity. Our findings suggest that the pFRG comprises a neuronal population that is involved in the primary respiratory rhythm generation in the rostrocaudally extending respiratory neuron network of the medulla.

Key words: **respiratory rhythm; optical imaging; voltage-sensitive dye; ventral medulla; neonatal rat; *in vitro***

Introduction

The neural circuit generating respiratory rhythm in mammals is located in the medulla of the lower brainstem. The main groups of medullary respiratory neurons are thought to be distributed rostrocaudally in the ventrolateral parts of the medulla, and they play a role in respiratory rhythm and inspiratory pattern generation (Feldman, 1986; von Euler, 1986; Bianchi et al., 1995; Richter and Spyer, 2001). However, there are still arguments over the fundamental question of which parts of the ventrolateral medulla are essential for primary rhythm generation (Ballanyi et al., 1999; Richter and Spyer, 2001), and the initiation site of respiratory rhythm is still unknown. The brainstem–spinal cord preparation isolated from newborn rats preserves the neuron networks of the respiratory center essential for respiratory rhythm generation *in vitro* (Suzue, 1984; Ballanyi et al., 1999). For understanding the macroscopic behavior of the rostrocaudally extending respiratory neuron network in the medulla, optical recordings (Cohen and Lesher, 1986; Grinvald et al., 1988; Momose-Sato et al., 2001) can be very effective. Indeed, respiratory neuron network activity in the medulla of this preparation is detectable as an optical image by observation from the ventral surface after the preparation is stained with a voltage-sensitive dye (Tokumasu et al., 2001), but detailed analysis of the starting points of the rhythmic respiratory activity has been difficult because of an inadequate signal-to-noise ratio of the optical signals. In the present study, we used a new optical recording system (Tominaga et al., 2000) that provides for data acquisition by the summation of optical signals from a certain pretriggering point. The system allows us to analyze neuronal activity correlating to spontaneous activity used as trigger signals. In brainstem–spinal cord preparations stained with a voltage-sensitive dye, we measured optical signals from several seconds before to several seconds after the inspiratory phase using inspiratory motor nerve discharge as the trigger signal. We found that preinspiratory population activity occurs in the localized region ventrolateral to the facial nucleus. Partial bilateral electrical lesioning of this limited region caused a significant reduction in respiratory frequency, implying that the neuronal population in this area may be important in respiratory rhythm generation.

Materials and Methods

Preparation and staining. Wistar rats ($n = 43$), 0–1 d of age, were deeply anesthetized with ether until the nociceptive reflexes were abolished. Usually, respiratory movement halted temporarily at this level of anesthesia. The cerebrum was quickly removed by transection at the intercollicular level, and the brainstem and spinal cord were isolated according to methods described previously (Suzue, 1984; Onimaru et al., 1988). The brainstem was rostrally decerebrated between the VIth cranial nerve roots and the lower border of the trapezoid body. In some experiments, the caudal half of the pons was retained, attached to the facial nerve roots. The brainstem–spinal cord preparation was incubated in a modified Krebs solution (described below) containing a fluorescent voltage-sensitive dye (Tominaga et al., 2000), Di-4-ANEPPS or Di-2-ANEPEQ (Molecular Probes, Eugene, OR). In preliminary experiments, excessive staining with these dyes decreased respiratory frequency and changed the spatiotemporal pattern of respiratory neuron activity. Therefore, the concentration of dye and the incubation period were carefully adjusted so that there would be no significant reduction in respiratory frequency:

Received Sept. 10, 2002; revised Nov. 13, 2002; accepted Dec. 2, 2002.

This work was supported by grants-in-aid for Scientific Research from the Ministry of Education, Science, and Culture of Japan. We thank F. Kato, Y. Kubo, and K. Ballanyi for comments on this manuscript.

Correspondence should be addressed to Dr. Hiroshi Onimaru, Department of Physiology, Showa University School of Medicine, 1-5-8 Hatanodai, Shinagawa-ku, Tokyo 142-8555, Japan. E-mail: oni@med.showa-u.ac.jp.

 0270-6474/03/231478-09$15.00/0

30–45 min with 0.2 mg/ml Di-4-ANEPPS or 30–55 min with 50 μg/ml Di-2-ANEPEQ. After being stained, the preparation was placed with the ventral surface up in a 1 ml perfusion chamber, which was mounted on a fluorescence microscope (BX50WIF-2; Olympus Optical, Tokyo, Japan). The preparation was superfused continuously at 2–3 ml/min with a modified Krebs solution consisting of (in mM): 124 NaCl, 5.0 KCl, 1.2 KH_2PO_4, 2.4 $CaCl_2$, 1.3 $MgCl_2$, 26 $NaHCO_3$, and 30 glucose and equilibrated with 95% O_2 and 5% CO_2, pH 7.4, at 26–27°C.

Inspiratory motoneuron activity, which was used as the trigger signal for optical recordings, was monitored at the IVth cervical (C4) ventral root with a glass capillary suction electrode. This C4 activity is known to synchronize with discharges of phrenic nerves, which are derived from the C4 and C5 ventral roots (Suzue, 1984). The electrical signal was stored through a 0.5 Hz high-pass filter in digital memory together with the optical imaging data. The onset of inspiratory activity was defined by visual inspection as the steepest rising point immediately before a peak of C4 activity, the time at which most inspiratory neurons start to fire. The frequency of spontaneous inspiratory activity from the nerve roots (respiratory frequency) was 6.3 ± 1.7 min^{-1}, and the burst duration was 990 ± 170 msec ($n = 32$).

For antidromic activation of the facial nucleus, the facial nerve was stimulated through a glass capillary suction electrode by application of a 0.1 msec, 15–20 V single pulse. Electrical lesioning was performed through a tungsten electrode with a 30 μm tip diameter by applying a 100 msec, 20 μA pulse. The extent of the lesions was verified histologically in 100 μm transverse sections stained with neutral red.

Optical recordings. Neuronal activity in the preparation was detected as a change in fluorescence of the voltage-sensitive dye by means of an optical recording apparatus (MiCAM01; Brain Vision Inc., Tsukuba, Japan; see also Tominaga et al., 2000) through a 510–550 nm excitation filter, a dichroic mirror, and a 590 nm absorption filter (U-MWIG2 mirror unit; Olympus Optical) with a tungsten–halogen lamp (150 W) as the light source. The CCD-based camera head has an 8.4 × 6.5 mm^2 imaging area consisting of 180 × 120 pixels, with a maximum time resolution of 3.5 msec. Magnification of the microscope was adjusted to 2× (or 4×) in most experiments so that an area of 4.2 × 3.25 mm^2 (or 2.1 × 1.6 mm^2) was covered by the image sensor. In our preliminary experiments, we did not find clear differences in optical signals from different depths of focus ranging from 0 (surface) to 300 μm. Therefore, we focused the microscope objective on the ventral surface plane of the brainstem–spinal cord preparation or on the surface plane of the rostral cross section.

Most recordings were performed with an acquisition time of 20 msec. Fluorescence signals for 6.8 sec per trial, including 1.7 sec before the initiation of the inspiratory burst, were totaled and averaged 50–150 times; C4 inspiratory activity was used as the trigger. During recordings, the respiratory frequency was not changed significantly, so the photodynamic toxicity was negligible. The fluorescence changes were expressed as a ratio (percentage, fractional changes) (i.e., the fluorescence intensity against that of the reference image). The differential image, processed with a software-spatial filter for 2 × 2 pixels, was represented by a pseudocolor display in which red corresponded to a fluorescence decrease, meaning membrane depolarization. For representation of the time course of the fluorescence change in the region of interest, optical signals were inverted. As discussed previously (Tokumasu et al., 2001), optical signals corresponding to spontaneous respiratory neuron activity were thought to reflect fluorescence changes primarily accompanying the subthreshold membrane depolarization (i.e.; respiration-related excitatory drive potential) in the soma but not each action potential in the soma or axon during burst activity.

Membrane potential recordings of respiratory neurons. Membrane potentials of respiratory neurons in the rostral ventrolateral medulla (RVLM) were recorded by means of conventional whole-cell patch-clamp methods (Onimaru and Homma, 1992). The patch pipette solution contained (in mM): 120 K-gluconate, 1 $CaCl_2$, 1 $MgCl_2$, 10 EGTA, 2 Na_2-ATP, and 10 HEPES as well as 0.5% Lucifer yellow (LY), pH 7.3. The membrane potentials were recorded with a single-electrode voltage-clamp amplifier (CEZ-3100; Nihon Kohden, Tokyo, Japan) after compensation for the series resistance (25–50 MΩ) and capacitance. In the present study, we recorded membrane potentials from three types of respiratory neurons: preinspiratory neurons (Pre-I neurons) showing membrane depolarization leading to the initiation of spike discharge by up to several hundred milliseconds before the onset of inspiratory C4 activity, type I inspiratory neurons showing EPSPs before the onset as well as after the termination of inspiratory-related nerve bursts, and type II inspiratory neurons showing EPSPs and spike discharge only during the inspiratory phase (Onimaru and Homma, 1992, Ballanyi et al., 1999). Pre-I–I neurons, a subtype of type I inspiratory neurons, which show spike discharge before and during the inspiratory phase, were also recorded (Smith et al., 1990; Ballanyi et al., 1999). Spike discharge of the Pre-I neuron is usually inhibited during the inspiratory phase and appears again after the termination of the inspiratory burst, although there are subtypes with different burst patterns (Ballanyi et al., 1999). To compare fluorescence changes in the optical recordings with the membrane potential trajectory, we averaged membrane potentials for 20–30 respiratory cycles (with a sampling rate of 0.2 or 1 kHz) using C4 activity as the trigger. For study of the location and morphological properties of neurons stained with LY, preparations were fixed for >48 hr at 4°C in Lillie solution (10% formalin in phosphate buffer, pH 7.0), rinsed with 15% sucrose–0.1 M phosphate buffer, pH 7.2, and incubated overnight in sucrose solution. Transverse 70 μm frozen sections were then cut with a cryostat. The intracellularly LY-marked neurons were reconstructed with the aid of a camera lucida attached to a fluorescence microscope (Olympus Optical).

Values are presented as means ± SD. Significance values ($p < 0.05$) were determined with a Student's *t* test.

Results

Optical image of respiratory neuron activity in the ventral medulla

Typical examples of optical images obtained by the ventral approach are shown in Figures 1 and 2. The optical records showed neuronal activity preceding, by ~500–600 msec, the inspiratory activity that started in the limited region of the RVLM, 1.3–1.6 mm lateral to the midline and extending rostrally from the level of the Xth cranial nerve roots (Figs. 1, *second frame*, 2*B*,*B*′). Activity then spread caudally and medially in the ventrolateral medulla and some also more rostrally during the preinspiratory phase (Fig. 1, *second* and *third frames*). Activity in the RVLM reached its peak immediately before a peak of C4 inspiratory activity and then decreased during the inspiratory phase (Fig. 2*B*′). During the inspiratory phase, plateau activity appeared in the more caudal ventrolateral medulla at the level of the most rostral roots of the XIIth cranial nerve and in the ventral horns of the cervical cord. Moreover, fluorescence changes in the caudal medulla and in the ventral horns were detected 100–300 msec before the onset of inspiratory activity, with a smaller amplitude than that of the RVLM. This spatiotemporal pattern of respiratory neuron activity in the medulla was confirmed in all other preparations examined ($n = 31$). We also confirmed this in optical recordings by data acquisition with a longer pretriggering period (3.4 sec before inspiratory activity).

We focused on the analysis of neuron activity, especially in the RVLM. The average duration of activity in the preinspiratory phase in the RVLM was 370 ± 170 msec (range, 75–700 msec; $n = 32$), which was 3.5% of the respiratory cycle period. The preinspiratory phase may be shorter if activity of more rostral nerve roots such as C1 or the XIIth cranial nerve is used as the trigger signal instead of C4, because the onset of the inspiratory activity of these nerves precedes that of phrenic motoneurons (Smith et al., 1990). The optical signals in the RVLM preceding inspiratory activity were thought to reflect activity of the Pre-I neurons in this area (Onimaru et al., 1987, 1988; Arata et al., 1990). Therefore, we compared the pattern of optical signals with membrane potential

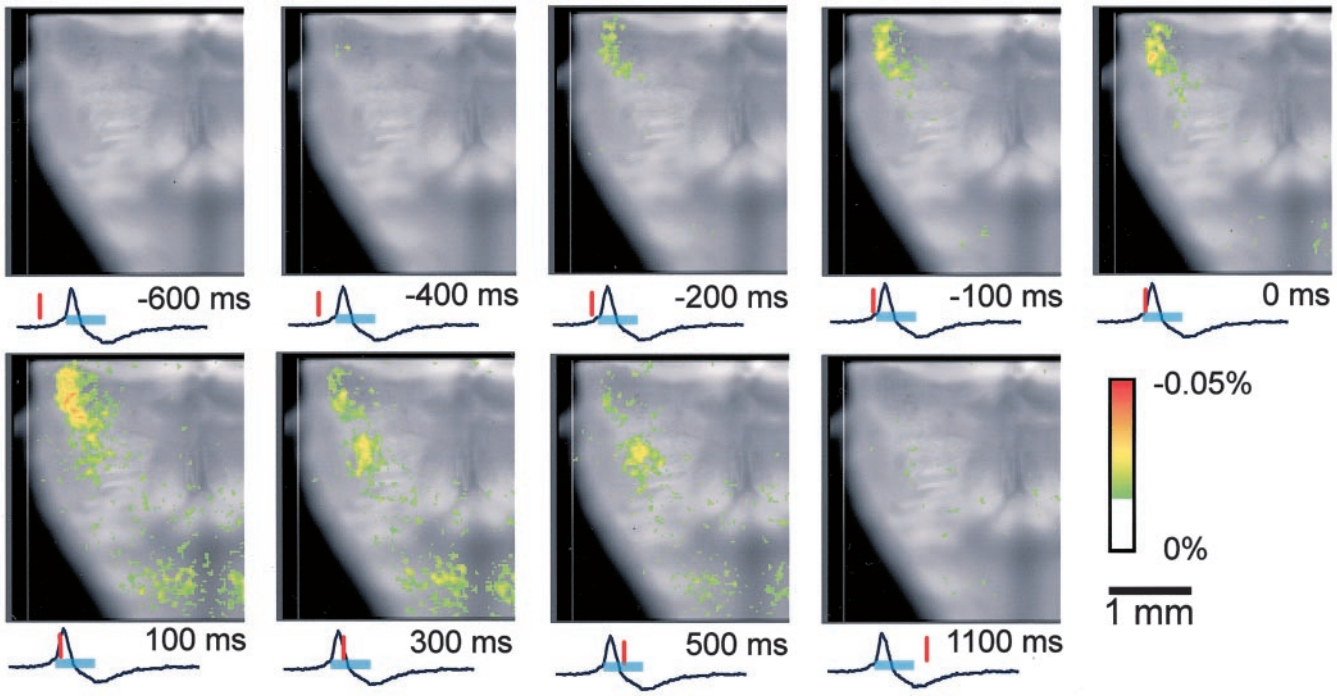

Figure 1. Spatiotemporal pattern of respiratory neuron activity observed on optical images. The image is superimposed on the ventral surface of the right half of the medulla. Also see Figure 2 for the orientation of the preparation. The *numbers* at the *bottom right* of each image denote the time from the start of C4 inspiratory activity. The *tracing* under each image is the C4 activity; the inspiratory phase is indicated by the *light-blue bar*. The *red vertical line* on the C4 tracing shows the time at which the image was obtained. Results are the average of 100 respiratory cycles triggered by C4 inspiratory activity. The preparation was stained with 50 μg/ml Di-2-ANEPEQ for 40 min. The sampling clock is 20 msec. Note that optical signals reflecting respiratory neuron activity appear in the RVLM during the preinspiratory phase. During the inspiratory phase, peak activity appears in the more caudal ventrolateral medulla.

trajectories that were recorded from Pre-I neurons in the RVLM of the same preparation after the optical recordings ($n = 9$). The Pre-I neuron shown in Figure 2*C* exhibited a long preinspiratory phase and a short postinspiratory phase in >80% of the respiratory cycles. The period for which optical signals were detected preceding the inspiratory phase corresponded well to the period of time for which the Pre-I neuron depolarized ~4 mV (see below) from the resting potential level (Fig. 2*C*, *average*). In three optical recordings, postinspiratory activity was also clearly detected (Fig. 2*D*), whereas the activity was less conspicuous than that during the preinspiratory phase in other preparations. The results indicate that neuron activity during the postinspiratory phase is less stable than that of the preinspiratory phase.

In nine Pre-I neurons recorded after optical recordings, preinspiratory membrane depolarization in the averaged trajectory was detectable as early as 1240 ± 310 msec preceding the inspiratory onset. Detectable changes in fluorescence during the preinspiratory phase in the optical recordings of the same preparations appeared as early as 620 ± 70 msec before the inspiratory onset. It is reasonable that there would be a difference in the period between detectable membrane potential change and detectable fluorescence change during the preinspiratory phase, because optical detection may require a certain threshold voltage change in weak signal intensity (e.g., spontaneous activity). We estimated this threshold voltage to be ~4 mV, because the period indicating subthreshold depolarization >4 mV from the resting level during the preinspiratory phase was 590 ± 150 msec in the averaged membrane potential trajectory. We also recorded membrane potentials from seven inspiratory neurons in the RVLM area similar to the Pre-I neuron recording site after optical recordings. Figure 3 shows examples of the averaged membrane potential trajectory of a typical Pre-I–I neuron (as an example of an inspiratory neuron with prolonged preinspiratory activity), a Pre-I neuron (Fig. 3*A*), and type II inspiratory neuron (Fig. 3*B*) together with fluorescence changes in the previously performed optical recordings in the same preparation. These and other recordings showed that fluorescence changes in the rostral medulla had fairly good correlation with membrane potential trajectories of Pre-I neurons, whereas those in the caudal medulla fit better with those of the inspiratory neurons.

The RVLM area in which strong preinspiratory optical signals were detected seems to overlap laterally with the facial nucleus. We confirmed this anatomically by examining the level of the facial nucleus in 100 μm serial sections dissected from the preparations. Furthermore, we confirmed the location by superimposing the active area on the optical images of the facial nucleus activated antidromically by facial nerve stimulation ($n = 5$). The active area was thought to correspond to the entire anatomical location of the ventral part of the facial nucleus. The result clearly showed that the main active area during the preinspiratory phase overlapped to the lateral edge of the facial nucleus (Fig. 4).

Optical signals and respiratory neurons in the ventral superficial region of the rostral medulla

One major technical problem of this optical measurement method is how to determine the depth of the location for neurons from which optical signals originate. We approached this problem by first examining the depth of diffusion of the voltage-sensitive dye into the tissue by transversely dissecting the rostral medulla after the preparation was stained (50 μg/ml Di-2-ANEPEQ, 45–50 min). We then observed the cut surface, monitoring C4 inspiratory activity. In these experiments ($n = 5$), optical signals corresponding to respiratory activity were detected with 0.013% fractional change even at a depth of 500 μm from

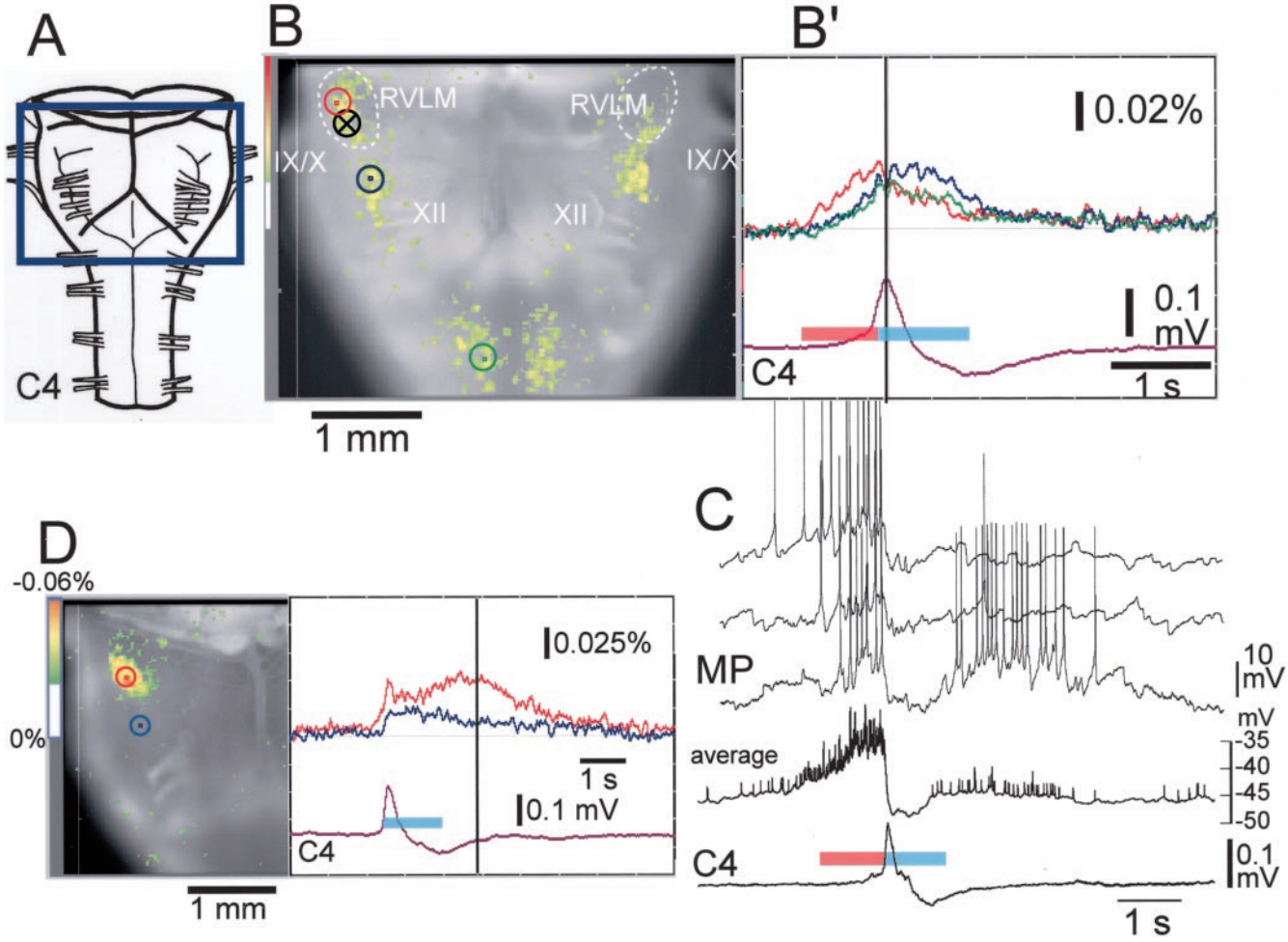

Figure 2. Fluorescence changes in the optical recording and electrophysiological recordings of respiratory neuron activity. The preparation is the same as in Figure 1 except for *D*. *A*, Ventral aspect of the preparation and the optical image recording area *boxed* in *blue*. *B*, Optical image of respiratory neuron activity near the C4 peak (at *dark vertical line* in *B'*) superimposed on the ventral surface of the medulla. *IX/X, XII*, Cranial nerves; *white dotted lines*, approximate area of the RVLM; *B'*, Fluorescence changes at three different points indicated by *dots* in *red*, *blue*, and *green circles* on *B*: *red*, in the RVLM at the level just rostral to the IX/Xth cranial roots; *blue*, in the more caudal ventrolateral medulla at the level of the rostral roots of the XIIth cranial nerve; and *green*, in the ventral horns of the cervical cord. Fluorescence decrease (i.e., depolarization) is upward. *C4*, Electrical record of C4 inspiratory activity. The *red bar* and *light-blue bar* on the C4 tracing denote the preinspiratory and inspiratory phases, respectively. Note that the fluorescence change precedes the inspiratory phase in all of the areas indicated, whereas the amplitude is larger in the RVLM (*red tracing*). *C*, Membrane potential trajectory (*MP*) of a Pre-I neuron recorded in the ventrolateral medulla 1.4 mm lateral to the midline and at the level of the IX/Xth roots of the same preparation (*circle with cross* in *B*). Three membrane potential traces are shown, one below the other. The averages of the membrane potential trajectory and C4 activity for 21 respiratory cycles are also shown (*average*, *C4*). The *red bar* and *light-blue bar* on the average C4 tracing denote the preinspiratory and inspiratory phases, respectively. *D*, An example exhibiting clear postinspiratory activity. *Left*, Optical image of respiratory neuron activity in the postinspiratory phase (*dark vertical line* at *right*) superimposed on the ventral surface of the right-side medulla. *Right*, Fluorescence changes at two different points indicated by *dots* in *red* and *blue circles* on the *left image*: *red*, in the RVLM at the level just rostral to the IX/Xth cranial roots; and *blue*, in the more caudal ventrolateral medulla near the level of the rostral roots of the XIIth cranial nerve. Results are the average of 100 respiratory cycles triggered by C4 inspiratory activity. The preparation was stained with 0.2 mg/ml Di-4-ANEPPS for 30 min. The sampling clock is 25 msec. Note the short (75 msec) preinspiratory activity and long (~2 sec) postinspiratory activity.

the ventral surface, where the dye concentration was reduced to ~60% of that of the ventral superficial region (data not shown). The results indicated that the dye diffused into the tissue at a concentration sufficient to allow for the detection of spontaneous neuron activity at a depth of 500 μm. This is considered the maximum depth for the detection of spontaneous neuron activity in the present system, because the fluorescence from such a deep region might be weakened because of tissue lying in the emission light path in the approach from the ventral surface.

Respiratory neurons may also be located in regions of the medulla that are deeper than the detectable depth by the ventral approach. Thus, to view respiratory neuron activity in the RVLM from a different direction, we observed the cut surface of the medulla stained with a voltage-sensitive dye after transverse sectioning at the rostral medulla ($n = 5$). The optical image showed that neuron activity started at the limited region ventrolateral to the facial nucleus and close to the ventral surface during the preinspiratory phase and then propagated medially and dorsally during the inspiratory phase (Fig. 5*A*). Major activity during the inspiratory phase overlapped to the facial nucleus. Thus, the optical recordings in the region of the facial motor nucleus from the ventral approach (Fig. 4) may in part reflect that of facial motoneurons, although the signal was rather weak, probably because of the difficulty in detecting activity from deeper cells. These observations suggest that the major cluster of neurons active during the preinspiratory phase is distributed close to the ventral surface such that the optical signals are detectable by the ventral approach. This was also supported by the fact that with comparatively weak staining with voltage-sensitive dye (e.g., for 40 min with 0.1 mg/ml Di-4-ANEPPS), the optical signals were detected

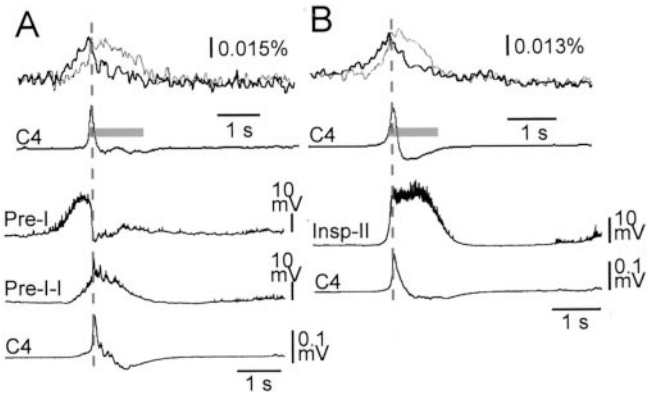

Figure 3. Comparison between fluorescence changes in optical recordings and averaged membrane potential trajectories of different types of respiratory neurons. *A, B, top*, Fluorescence changes at two different points similar to Figure 2 *B* or *D*: *thick line*, in the RVLM at the level just rostral to the IX/Xth cranial roots; *thin line*, in the more caudal ventrolateral medulla near the level of the rostral roots of the XIIth cranial nerve. Results are the average of 50 (in *A*) or 100 (in *B*) respiratory cycles triggered by C4 inspiratory activity. Fluorescence decrease (i.e., depolarization) is upward. The preparation was stained with 50 μg/ml Di-2-ANEPEQ for 45 min in *A* or 43 min in *B*. The sampling clock is 20 msec. *Gray bars* on the average C4 tracing (*C4*) denote the inspiratory phase. *A, B, bottom*, Averaged membrane potential trajectories from a Pre-I neuron, a Pre-I–I type inspiratory neuron, and a type II inspiratory neuron (*Insp-II*), recorded in the ventrolateral medulla 1.3–1.4 mm lateral to the midline and at the level of the IX/Xth roots. *C4*, Averaged C4 activity. The *vertical dotted lines* in *A* and *B* denote the time of peak C4 activity.

primarily in the RVLM, in contrast to weak signals coming from the caudal ventrolateral medulla (data not shown). That is, a longer incubation time (or a higher dye concentration) for the staining was required for clear detection of optical signals in the caudal ventrolateral medulla during the inspiratory phase compared with those in the RVLM during the preinspiratory phase.

To confirm the detailed location of Pre-I neurons in the region ventrolateral to the facial nucleus, we marked them with LY and plotted them after whole-cell patch-clamp recordings. Pre-I neurons were found in the reticular formation ventrolateral to the facial nucleus as well as in the ventrolateral edge of the facial nucleus (Fig. 5*C*,*D*). The resting membrane potential ranged from −47 to −55 mV (−49.2 ± 2.5 mV; $n = 11$), and the input resistance was 443 ± 328 MΩ. During the recording procedure, we also found five inspiratory neurons and two expiratory neurons in the same region, but we did not analyze their electrophysiological properties in detail.

Effects of partial electrical lesioning in the RVLM

For help in evaluating the functional role of the respiratory neuron group in the RVLM, we examined the effects of partial electrical lesioning of the limited area in the RVLM in which the strong fluorescence change was detected before the onset of inspiratory activity. After unilateral lesioning, the fluorescence change in the contralateral RVLM was still seen clearly during the preinspiratory phase (Fig. 6*B*). This optical signal was markedly depressed (<12% of control) after subsequent partial lesioning of the remaining side (Fig. 6*C*). Thus, after partial, bilateral lesioning of the RVLM, major fluorescence changes were detected only during the inspiratory phase in the caudal ventrolateral medulla at the most rostral level of the XIIth cranial nerve and in the ventral horn of the cervical cord. We confirmed that these lesioned areas were limited in the superficial ventrolateral medulla to the facial nucleus (Fig. 6*D*). The C4 burst rate did not decrease with unilateral lesioning (5.7 ± 1.6/min in control; 5.5 ± 1.9/min after unilateral lesioning; $n = 8$). In the preparations that indicated a relatively irregular C4 rhythm in the control (Fig. 6*A*), the rhythm became more stable after unilateral lesioning. Then subsequent partial lesioning of the other side caused a significant decrease in the C4 rate (2.1 ± 0.7/min; $p < 0.001$; 10–15 min after the lesioning). The burst duration of C4 activity was 990 ± 210 msec in control, 760 ± 138 msec after unilateral lesion, and 1110 ± 298 msec after partial bilateral lesioning. The decrease in burst duration after unilateral lesioning was not significant; the increase after bilateral lesioning was significant ($p < 0.05$) compared with that after unilateral lesioning.

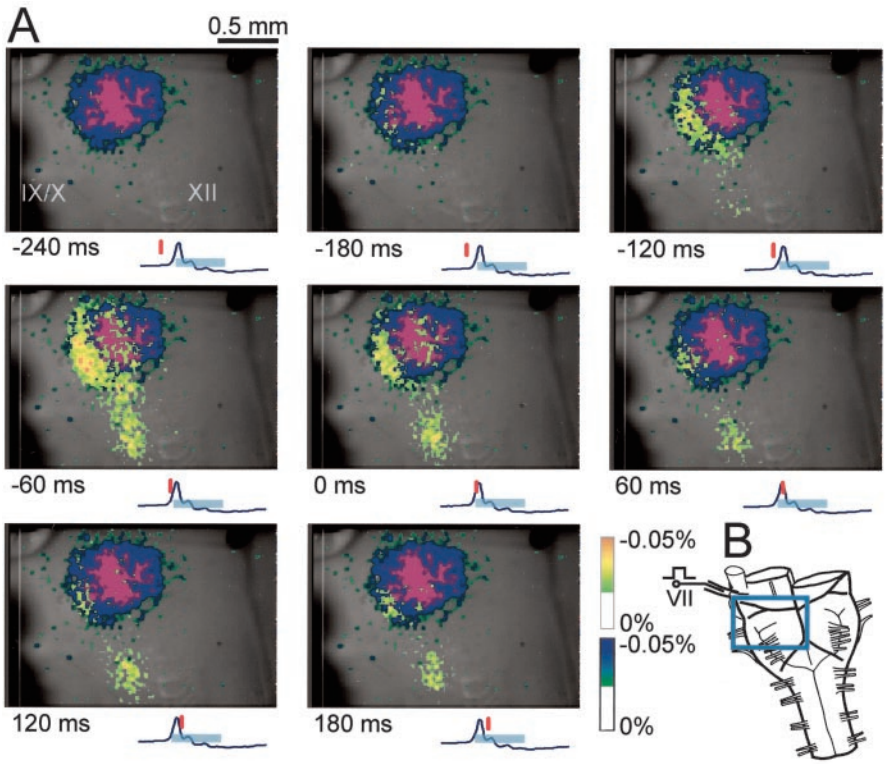

Figure 4. Optical images of respiratory neuron activity superimposed on the area of the facial nucleus. *A*, The *dark blue* area in each image indicates the facial nucleus of the right side of the medulla, which was activated antidromically by stimulation of the right facial nerve. *Purple* denotes a fluorescence change below -0.05%. The *numbers* at the *bottom left* of each image denote the time from the start of C4 inspiratory activity. The *tracing* under each image is the C4 activity; the inspiratory phase is indicated by the *light-blue bar*. The *red vertical line* on the C4 tracing shows the time at which the image was obtained. The preparation was stained with 50 μg/ml Di-2-ANEPEQ for 40 min. Results are the average of 50 respiratory cycles triggered by C4 inspiratory activity. The sampling clock is 30 msec. Note that optical signals during the preinspiratory phase appear to overlap to the lateral edge of the facial nucleus. *IX/X, XII*, Cranial nerves. *B*, Diagram of the ventral aspect of the preparation and the optical image recording area *boxed* in *blue*. *VII*, Facial nerve.

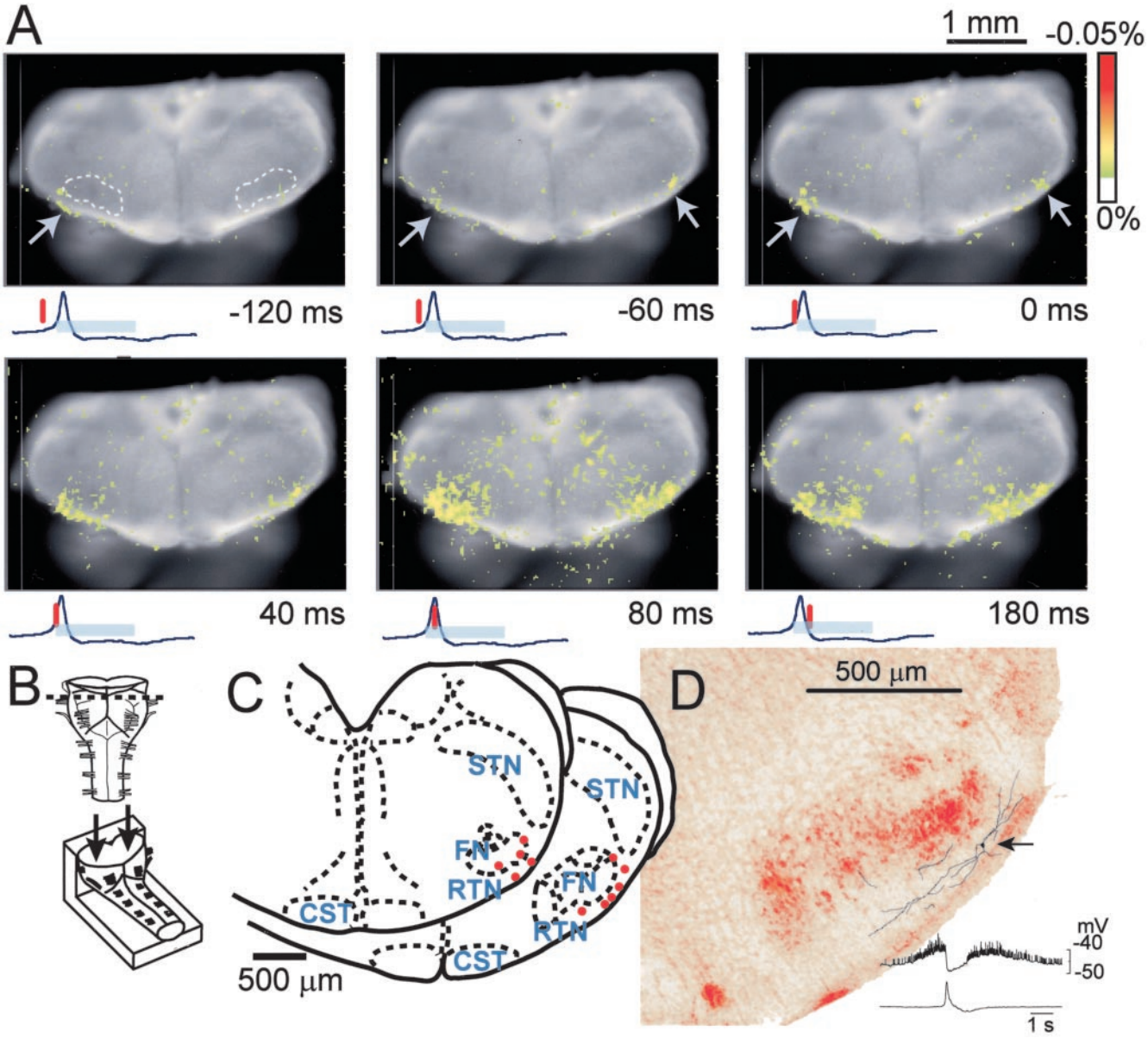

Figure 5. Optical images of respiratory neuron activity obtained by observation from the cut surface of a cross section of the rostral medulla. *A*, Spatiotemporal pattern of optical images of respiratory neuron activity superimposed on the cut surface of the rostral medulla. The *numbers* at the *bottom right* of each image denote the time from the start of C4 inspiratory activity. The *tracing* under each image is the C4 activity; the inspiratory phase is indicated by the *light-blue bar*. The *vertical red line* on the C4 tracing shows the time at which the *top image* was obtained. Results are the average of 100 respiratory cycles triggered by C4 inspiratory activity. The sampling clock is 20 msec. Note that optical signals reflecting respiratory neuron activity appear in the part ventrolateral to the facial nucleus (*top left*, *white dotted line*) during the preinspiratory phase (*arrows*). *B*, Schematic representation of the preparation. The preparation was cut transversely at the level (indicated by a *dotted line*) rostral to the IX/Xth cranial nerve roots and then stained with 0.1 mg/ml Di-4-ANEPPS for 56 min. It was then fixed onto a rubber block with pins and cut surface up, for observation from the cut surface of the cross section (*arrows*). *C*, Pre-I neurons in the part ventrolateral to the facial nucleus. The neuron activities were recorded in the whole-cell configuration in the same type of preparations as illustrated in *B* by approaching from the rostral cut surface. *Red dots* indicate locations of recorded neurons. Neurons were found in the reticular formation ventrolateral to the facial nucleus, and some neurons were also found in the ventrolateral edge of the facial nucleus. *Dotted lines* indicate demarcation between some anatomical structures. *FN*, Facial nucleus; *CST*, corticospinal tract; *STN*, spinal trigeminal nucleus, oral part. *D*, An example of reconstruction of a Pre-I neuron stained with LY. The *arrow* denotes the site of soma located ventrolateral to the facial nucleus. The axon could not be traced. The averaged membrane potential trajectory is shown in the *bottom right* with C4 activity.

Discussion

Technical limitations

The basic ability of the present optical recording system to measure neuron activity is described in detail by Tominaga et al. (2000). Here, we discuss only specific technical problems for measuring respiratory neuron activity in the brainstem preparation. The amplitude of optical signals likely depends on many factors: the type of preparation (especially its transparency), the concentration of dye in the tissue, and the density of active (synchronized) neurons (for review, see Grinvald et al., 1988). In the present study, we examined the depth of diffusion of the voltage-sensitive dye into the tissue by observing the cut surface of a transverse section at the rostral medulla after the preparation was stained. The results suggested that the spontaneous neuron activity that was detectable in the ventral approach must be at a depth <500 μm from the ventral surface. Therefore, our measurement may not detect neuron activity in deeper regions. Moreover, it should be noted that optical signals from superficial cells could be

detected with larger amplitude and earlier onset than those from deeper cells, even if these cells were active over a similar time course. Thus, staining with voltage-sensitive dye for a longer time or with a higher concentration of dye is required for the detection of neuron activity in deeper regions (for example, inspiratory neuron activity in the caudal medulla versus Pre-I neuron activity in the rostral medulla; see below). However, the staining process should be carefully controlled, because excessive staining actually depresses neuron activity (Grinvald et al., 1988; our unpublished observation). On the basis of comparison between averaged membrane potential trajectory and optical signals, we presumed that the present system could detect a subthreshold membrane potential change (of spontaneously bursting–medullary respiratory neurons) of >4 mV as an optical signal.

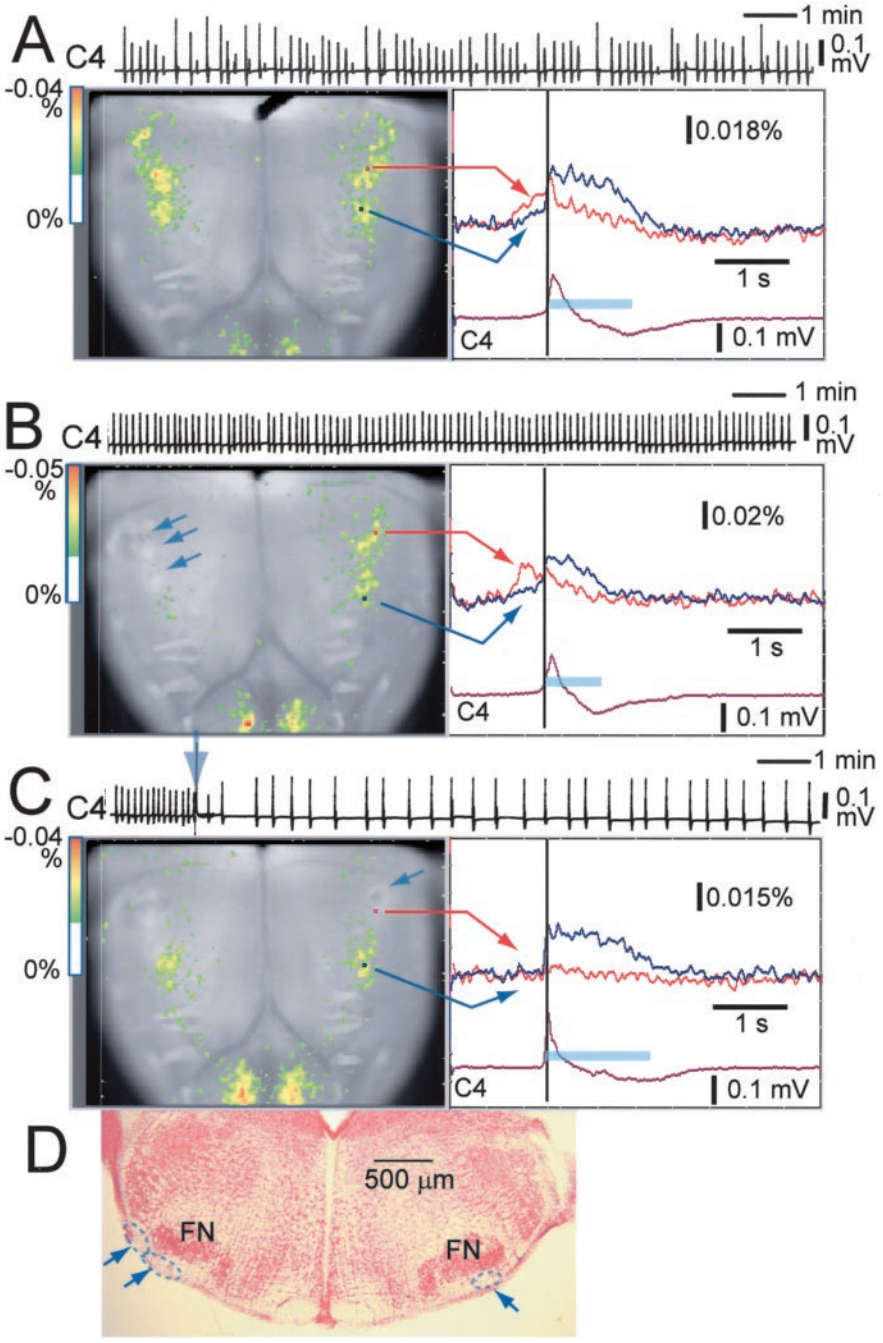

Figure 6. Effects of partial electrical lesioning of the RVLM on C4 rhythm and spatiotemporal pattern of respiratory neuron activity. *A*, C4 activity and optical records in control. *B*, C4 activity and optical records after partial lesioning of three points (*arrows*) in the right side of the RVLM. *C*, C4 activity and optical records after subsequent partial lesioning of a point (*arrow*) in the left side of a similar rostral medulla. *C4*, Inspiratory C4 activity. *A–C, left*, Optical images of respiratory neuron activity near the C4 onset (*dark vertical line* at *right*) superimposed on the ventral surface of the medulla. *A–C, right*, Fluorescence changes at two points indicated on each *right panel*: *red*, in the RVLM at the level just rostral to the IX/Xth cranial roots; *blue*, in the more caudal ventrolateral medulla at the level of the rostral roots of the XIIth cranial nerve; the inspiratory phase is indicated by the *light-blue bar*. Fluorescence decrease (i.e., depolarization) is upward. The preparation was stained with 50 μg/ml Di-2-ANEPEQ for 50 min. Results are the average of 50 respiratory cycles triggered by C4 inspiratory activity. The sampling clock is 20 msec. Note that preinspiratory activity recorded optically in the intact side is still clearly observed after partial lesioning of the right side of the rostral medulla (*B*). After subsequent partial lesioning of the other side, preinspiratory activity recorded optically is markedly depressed and the C4 rate is reduced (*arrow* on the C4 record), whereas the duration of inspiratory activity in the caudal medulla as well as that of C4 activity are prolonged. *D*, Histological verification of the electrical lesioning; 100 μm transverse section. The lesions indicated by *dotted lines* and *arrows* are confirmed in the limited area ventrolateral to the facial nucleus (*FN*).

Spatiotemporal pattern of respiratory neuron activity in the ventral medulla

The present optical recording study clearly localized respiration-related activity to the limited region of the RVLM, ventrolateral to the facial nucleus, which was characterized by a change in fluorescence preceding the inspiratory burst. We found that the fluorescence change during the preinspiratory phase in this area correlated well with the averaged membrane potential trajectory of Pre-I neurons, suggesting that the optical signal reflects Pre-I neuron activity in this area. On the contrary, many Pre-I neurons are repolarized with varied strength during the inspiratory phase (Onimaru and Homma, 1992). Therefore, the activity of Pre-I neurons exhibiting only minor repolarization during the inspiratory phase may contribute to the optical signal in the RVLM during the inspiratory phase; the signal appeared with a decrease to only a certain level. In addition, the optical signals may also reflect inspiratory neuron activity in this area. We confirmed that Pre-I neurons as well as inspiratory neurons were located in the superficial region ventrolateral to the facial nucleus. Thus, we propose to refer to this respiratory neuron group as the para-facial respiratory group (pFRG). Although precise identification of the anatomical structure of the pFRG remains for future study, the medial part of the pFRG may overlap to the retrotrapezoid nucleus (RTN), which has been identified in the cat and the rat as an area in which neurons with projections to the ventral respiratory group (VRG) are found (Smith et al., 1989; Ellenberger and Feldman, 1990; Nunez-Abades et al., 1993) and the presence of respiratory neurons are reported (Pearce et al., 1989; Connelly et al., 1990). Because recent studies have suggested that the RTN plays a

role in central chemoreception (Bodineau et al., 2000; Nattie, 2001), the pFRG may receive tonic drive from central chemoreceptors. The major population of the pFRG seems to be lateral to the RTN, although it was originally described to extend more laterally at rostral levels of the facial nucleus (Smith et al., 1989). Therefore, it is important to determine whether the pFRG neurons project directly to the VRG. The caudal part of the pFRG overlaps to the rostral part of the ventrolateral medulla, which has been examined electrophysiologically in previous studies (i.e., the ventral part of the retrofacial nucleus near the caudal end of the facial nucleus) (Onimaru et al., 1987; Arata et al., 1990). Thus, the present findings show that the respiratory activity in the rostral medulla extends more rostrally and laterally than known previously.

During the inspiratory phase, corresponding plateau activity appeared in a region more caudal and medial than the pFRG. This optical signal may primarily reflect activity of an inspiratory neuron group close to the ventral surface near this level of the medulla, as shown in Figure 13 of Smith et al. (1990). The caudal inspiratory activity became more conspicuous with longer voltage-sensitive dye staining than in the case of pFRG. This suggests that the distribution of neurons active during the inspiratory phase in the caudal medulla extends to a deeper region below the ventral surface. Fluorescence changes of small amplitude were also detected 100–300 msec before the onset of inspiratory activity in the caudal medulla. Such signals possibly reflect activity of type I inspiratory neurons (Onimaru and Homma, 1992) and also some Pre-I neurons in this area (Arata at al., 1990; Smith et al., 1990). This caudal area may correspond to the level of (or slightly rostral to) the preBötzinger complex, which has attracted attention recently as the proposed kernel of respiratory rhythm generation (Smith et al., 1991; Rekling and Feldman, 1998; see below).

Functional considerations

There are a substantial number of studies suggesting that neurons in the preBötzinger complex are necessary and sufficient for the generation of respiratory-related motor rhythms (Smith et al., 1991; Rekling and Feldman, 1998; Koshiya and Smith, 1999). There are also neurons in the preBötzinger complex that exhibit prominent preinspiratory depolarization and spike activity in both the presence and absence of the pFRG (Del Negro et al., 2001). *In vivo* selective lesioning of the preBötzinger complex neurons with neurokinin-1 receptors disrupts the rhythm, indicating that this area is crucial for rhythm generation *in vivo* (Gray et al., 2001). It has been shown that respiratory rhythm persists in the brainstem–spinal cord preparation after removal of the pFRG but not after removal of the preBötzinger complex (Smith et al., 1991). Moreover, slice preparations from the caudal medulla including the preBötzinger complex (but not the pFRG) produce respiratory-like neuronal bursts (Smith et al., 1991). However, McLean and Remmers (1994) reported that transection of the medulla just caudal to the Xth cranial nerve root, corresponding to the caudal border of the pFRG, significantly decreased the burst frequency. We also confirmed this in the experiments combined with optical recordings (our unpublished observations).

The optical images in the present study revealed that respiratory neuron activity appeared first from the pFRG in the rostrocaudally extending respiratory neuron network in the ventral medulla. However, this finding itself does not necessarily mean that the pFRG functions as the initiation site of respiratory rhythm. For instance, it is possible that neurons in the pFRG exhibit their activity as a result of receiving excitatory input from other neuron groups located outside the area in which the activity could be detected with the present optical recording. Nevertheless, partial bilateral lesioning of the pFRG area caused a significant reduction in the respiratory rate together with changes in the spatiotemporal pattern of the respiratory neuron activity. This supports the notion that the pFRG plays an important role in respiratory rhythm generation. Previous studies have shown that bilateral lesions in the caudal ventrolateral medulla, which seems to be identical to the active caudal area revealed in the present optical recording, cause inspiratory activity to disappear, whereas the rhythmic burst of Pre-I neurons in the more rostral medulla was preserved (Onimaru et al., 1988). Consequently, it is possible that rhythmically active Pre-I neurons in the pFRG interact with preBötzinger complex neurons as a coupled oscillator system to regulate the rhythm of the intact system.

References

Arata A, Onimaru H, Homma I (1990) Respiration-related neurons in the ventral medulla of newborn rats in vitro. Brain Res Bull 24:599–604.

Ballanyi K, Onimaru H, Homma I (1999) Respiratory network function in the isolated brainstem–spinal cord of newborn rats. Prog Neurobiol 59:583–634.

Bianchi AL, Denavit-Saubie M, Champagnat J (1995) Central control of breathing in mammals: neuronal circuitry, membrane properties, and neurotransmitters. Physiol Rev 75:1–45.

Bodineau L, Cayetanot F, Frugiere A (2000) Possible role of retrotrapezoid nucleus and parapyramidal area in the respiratory response to anoxia: an in vitro study in neonatal rat. Neurosci Lett 295:67–69.

Cohen LB, Lesher S (1986) Optical monitoring of membrane potential: methods of multisite optical measurement. In: Optical methods in cell physiology (De Weer P, Salzberg BM, eds), pp 71–99. New York: Wiley.

Connelly CA, Ellenberger HH, Feldman JL (1990) Respiratory activity in retrotrapezoid nucleus in cat. Am J Physiol 258:L33–L44.

Del Negro CA, Johnson SM, Butera RJ, Smith JC (2001) Models of respiratory rhythm generation in the pre-Bötzinger complex. III. Experimental tests of model predictions. J Neurophysiol 86:59–74.

Ellenberger HH, Feldman JL (1990) Brainstem connections of the rostral ventral respiratory group of the rat. Brain Res 513:35–42.

Feldman JL (1986) Neurophysiology of breathing in mammals. In: Handbook of physiology. The nervous system. Intrinsic regulatory systems of the brain. Sect 1 (Bloom FE, ed), pp 463–524. Bethesda, MD: American Physiological Society.

Gray PA, Janczewski WA, Mellen N, McCrimmon DR, Feldman JL (2001) Normal breathing requires preBötzinger complex neurokinin-1 receptor-expressing neurons. Nat Neurosci 4:927–930.

Grinvald A, Frostig RD, Lieke E, Hildesheim R (1988) Optical imaging of neuronal activity. Physiol Rev 68:1285–1366.

Koshiya N, Smith JC (1999) Neuronal pacemaker for breathing visualized in vitro. Nature 400:360–363.

McLean HA, Remmers JE (1994) Respiratory motor output of the sectioned medulla of the neonatal rat. Respir Physiol 96:49–60.

Momose-Sato Y, Sato K, Kamino K (2001) Optical approaches to embryonic development of neural functions in the brainstem. Prog Neurobiol 63:151–197.

Nattie EE (2001) Central chemosensitivity, sleep, and wakefulness. Respir Physiol 129:257–268.

Nunez-Abades PA, Morillo AM, Pasaro R (1993) Brainstem connections of the rat ventral respiratory subgroups: afferent projections. J Auton Nerv Syst 42:99–118.

Onimaru H, Homma I (1992) Whole-cell recordings from respiratory neurons in the medulla of brainstem–spinal cord preparations isolated from newborn rats. Pflügers Arch 420:399–406.

Onimaru H, Arata A, Homma I (1987) Localization of respiratory rhythm-generating neurons in the medulla of brainstem–spinal cord preparations from newborn rats. Neurosci Lett 78:151–155.

Onimaru H, Arata A, Homma I (1988) Primary respiratory rhythm generator in the medulla of brainstem–spinal cord preparation from newborn rat. Brain Res 445:314–324.

Pearce RA, Stornetta RL, Guyenet PG (1989) Retrotrapezoid nucleus in the rat. Neurosci Lett 101:138–142.

Rekling JC, Feldman JL (1998) PreBötzinger complex and pacemaker neurons: hypothesized site and kernel for respiratory rhythm generation. Annu Rev Physiol 60:385–405.

Richter DW, Spyer KM (2001) Studying rhythmogenesis of breathing: comparison of in vivo and in vitro models. Trends Neurosci 24:464–472.

Smith JC, Morrison DE, Ellenberger HH, Otto MR, Feldman JL (1989) Brainstem projections to the major respiratory neuron populations in the medulla of the cat. J Comp Neurol 281:69–96.

Smith JC, Greer JJ, Liu G, Feldman JL (1990) Neural mechanisms generating respiratory pattern in mammalian brainstem–spinal cord in vitro. J Neurophysiol 64:1149–1169.

Smith JC, Ellenberger HH, Ballanyi K, Richter DW, Feldman JL (1991) Pre-Bötzinger complex: a brainstem region that may generate respiratory rhythm in mammals. Science 254:726–729.

Suzue T (1984) Respiratory rhythm generation in the in vitro brain stemspinal cord preparation of the neonatal rat. J Physiol (Lond) 354:173–183.

Tokumasu M, Nakazono Y, Ide H, Akagawa K, Onimaru H (2001) Optical recording of spontaneous respiratory neuron activity in the rat brain stem. Jpn J Physiol 51:613–619.

Tominaga T, Tominaga Y, Yamada H, Matsumoto G, Ichikawa M (2000) Quantification of optical signals with electrophysiological signals in neural activities of Di-4-ANEPPS stained rat hippocampal slices. J Neurosci Methods 102:11–23.

von Euler C (1986) Brainstem mechanisms for generation and control of breathing pattern. In: Handbook of physiology. The respiratory system. Sect 3 (Fishman AP, ed), pp 1–67. Bethesda, MD: American Physiological Society.